HOSTED BY
ELSEVIER

Contents lists available at ScienceDirect

Asian Pacific Journal of Tropical Medicine

journal homepage: http://ees.elsevier.com/apjtm

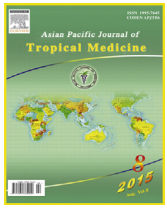

Original research http://dx.doi.org/10.1016/j.apjtm.2015.07.011

Renal blood perfusion in GK rats using targeted contrast enhanced ultrasonography

Bo Liu[2,#], Feng Liang[1,#], Li-Ping Gu[1,#], Chao-Qing Wang[2], Xing-Hua Li[1], Yi-Min Jiang[1], Wei-Mei Li[1], Qing-Zhi Guo[1], Fang Ma[1*]

[1]*Shanghai Jiao Tong University Affiliated Sixth People's Hospital, Shanghai 200233, China*

[2]*Xinxiang Medical College, Xinxiang, Henan 453003, China*

ARTICLE INFO

Article history:
Received 15 May 2015
Received in revised form 20 Jun 2015
Accepted 15 Jul 2015
Available online 22 July 2015

Keywords:
Targeted microbubble contrast agent
Contrast enhanced ultrasonography
Thrombomodulin
GK rats

ABSTRACT

Objective: To explore application of targeted contrast enhanced ultrasonography in diagnosis of early stage vascular endothelial injury and diabetic nephropathy.

Methods: Targeted SonoVue-TM microbubble was prepared by attaching anti-TM monoclonal antibody to the surface of ordinary microbubble SonoVue by biotin – avidin bridge method and ultrasonic instrument was used to evaluate the developing situation of targeted microbubble *in vitro*. Twenty 12-week-old male GK rats and 20 Wistar rats were enrolled in this study, and were randomly divided into targeted angiography group and ordinary angiography group. Targeted microbubbles SonoVue-TM or general microbubble SonoVue were rapidly injected to the rats via tail vein; the developing situation of the two contrast agents in rats kidneys was dynamically observed. Time-intensity curve was used to analyze rat kidney perfusion characteristics in different groups.

Results: Targeted ultrasound microbubble SonoVue-TM was successfully constructed, and it could be used to develop an external image. Targeted microbubbles SonoVue-TM enabled clear development of experimental rat kidney. Time-intensity curve shapes of rat kidney of the two groups showed as single apex with steep ascending and slowly descending branch. Compared with the control group, the rising slope of the GK rat renal cortex, medulla in targeted angiography group increased ($P < 0.05$); the peak intensity of medulla increased ($P < 0.05$), and the total area under the curve of medulla increased ($P < 0.05$). Compared with control group, the ascending branch of the GK rat in renal cortex, medulla in ordinary angiography group increased ($P < 0.05$). The peak intensity of the curve increased ($P < 0.05$), and the total area under the curve increased ($P < 0.05$). Compared with the ordinary angiography group, the peak of GK rat medulla curve in targeted angiography group intensity increased ($P < 0.05$), and the total area under the curve increased ($P < 0.05$).

Conclusions: Targeted microbubbles SonoVue-TM can make a clear development of experimental rat kidney, its stable performance meet the requirement of ultrasonic observation time limit, and it can reflect early changes of blood perfusion in GK rat kindey.

1. Introduction

Microvascular damage is the main pathological basis of diabetes mellitus [1]. It is reversible at the first stage, and become irreversible at the later stage, therefore, early intervention is of great importance to delay the progression of the disease [2–4]. At present, there has no intuitive and reliable diagnostic method to estimate the damage of microvascular [5]. Target imaging enables the target region imaged at the level of tissue and cell, so as to reflect the change of diseased tissue in a molecular aspect. Research shows that the injury of the structure and function of endothelial cell is the main cause of microangiopathy, and so we can estimate the early lesion of microvascular by evaluate the structure and function of endothelial cell. Thrombomodulin (TM), a kind of

*Corresponding author: Fang Ma, Shanghai Jiao Tong University Affiliated Sixth People's Hospital, Shanghai 200233, China.
Tel: +86 18017579071
E-mail: mafang59@126.com

Peer review under responsibility of Hainan Medical University.
Foundation project: It was supported by Shanghai Municipal Commission of Health and Family Health Planning Key Projects (NO. 20134023).

[#] These authors contributed equally to this work.

glycoprotein with anticoagulant activity that can regulate the inflammatory response, plays an important role in the proliferation of the cell and the progress of fibrinolysis [6,7]. The plasma soluble TM can be served as a molecular marker which can reflect the injury of vascular endothelial cells in patients with diabetes mellitus. Nowadays, there was no report of targeted ultrasound contrast agent to detect the injury of vascular endothelial. In this study, we build targeted ultrasound contrast agent by attaching TM monoclonal antibody to ultrasound microbubbles with biotin-streptavidin connectors, and explore the feasibility of the targeted ultrasound contrast agent in imaging the Goto-Kakizaki (GK rats) as well as observe the characteristics of renal blood perfusion. The finding can deepen our understanding to the pathogenesis of the endothelium dysfunction in diabetes mellitus, and provide new target point for the early intervention of diabetic complication.

2. Materials and methods

2.1. Materials

Sulfur hexafluoride microbubble was purchased from SonoVue, DSPE-PEG2000-Biotin was from Avanti Polar Lipids Inc, streptavidin was provided by Seebio Inc, Mouse anti-Human thrombomodulin Biotin-conjugated Antibody and Donkey Anti-Mouse IgG were purchased from United States Biological.

ESAOTE Technos MPX DU8 color Doppler ultrasonic cardiogram was from esaote.

2.2. Construction of targeted ultrasound microbubble

A tube of Sulfur Hexafluoride Microbubble ultrasonographic contrast agent and 3 mL PBS were blended together, shocked sufficiently to form a homogeneous microbubble suspension; 750 μL DSPE-PEG2000-Biotin (100 μg/mL) was added into the suspension, and then the liquid was reaction in a shaking table (55 rpm) at 37 °C for 1 h; the suspension was centrifuged at 4 °C for 10 min to separate the microbubble; the biotinylated ultrasound microbubble was obtained after washed for two times.

2.3. Identification and evaluation of targeted ultrasound microbubble

The culture dish (35 mm) was coated with streptavidin at the concentration of 2.5 μg/mL, washed with PBS for 3 times. The dish was blocked with 0.3% BSA at room temperature for 30 min, after washed with PBS for another 3 times, 9 mL PBS was added into the dishes, and 20 μL biotinylated ultrasound microbubble and 20 μL ordinary ultrasound microbubble was added into two dishes respectively, upside down the dishes, and reacted for 20 min at room temperature. Afterwards, 1 mL liquid was reserved in the dish, the number of the microbubble was counted under a microscope; 3 μg streptavidin per 1×10^7 mircrobubble was added into the dish, and then incubated on the ice for 30 min. After incubation, the sample was centrifuged, and washed with PBS, the purified biotinylated ultrasound microbubble coated with streptavidin was obtained. The microbubble was counted again, and 1.5 μg anti-TM antibody labeled by biotin per 1×10^7 microbubble was added, and then incubated on the ice for 30 min. After incubation, the sample was centrifuged, and washed with PBS, the targeted ultrasound microbubble (SonoVue-TM) was obtained. 5 μL Donkey Anti-Mouse IgG was blended with 500 μL SonoVue-TM suspension, and after reaction at cool dark place for 30 min, the microbubble was centrifuged, washed and collected for smear examination. SonoVue-TM microbubble and ordinary microbubble was added into eppendorf tube respectively, and checked with contrast ultrasound underwater.

2.4. Animal experiment

Rats were anesthetized with pentobarbital sodium (30 mg/kg), immobilized in the supine position, and the hair in the abdomen was shaved carefully. Puncture the caudal vein with a needle, and the needle was carefully fixed to prevent it from slipping. Imaging was conducted by using an Esaote Technos MPX DU8 color ultrasonographic device (Esaote, Italy). The probe was placed on the plank of the rat, and the position of the probe was adjusted after the clarity of the two-dimensional image, so that can obtain the largest long axis section of the kidney and make the renal cortex, medulla, and sinus display clearly. A total of 0.1 mL ordinary ultrasound microbubble and SonoVue-TM microbubble was injected into the caudal vein of rat respectively, and then washed with saline. The time intensity curve (TIC) analysis software was used to analyze the image.

2.5. Statistical analysis

In the study, SPSS 17.0 software was used for statistical analysis in this study. All data are expressed as mean ± SEM, and statistical significance was evaluated using Students's *t*-test. *P* values of 0.05 or less were considered significant.

3. Results

3.1. Characteristics of the material

The SonoVue-TM microbubble showed clear red fluorescence when viewed under a fluorescence microscope (Figure 1), which suggest that anti-TM antibody was attached to the SonoVue-TM microbubble successfully. The targeted microbubble can imagined *in vitro*, the intensity of the signal was similar with the regular microbubble (Figure 2).

3.2. Perfusion image of the rat kidney

SonoVue-TM microbubble enabled the kidney of the rat in every group showed clearly. Renal arterial and interlobar arterial were enhanced quickly in arborescent type, and then renal cortex showed homogenous enhancement, while medulla nephrica and

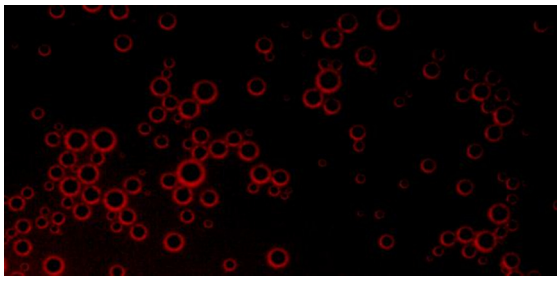

Figure 1. Targeted microbubble SonoVue-TM showing red fluorescence under a fluorescent microscope.

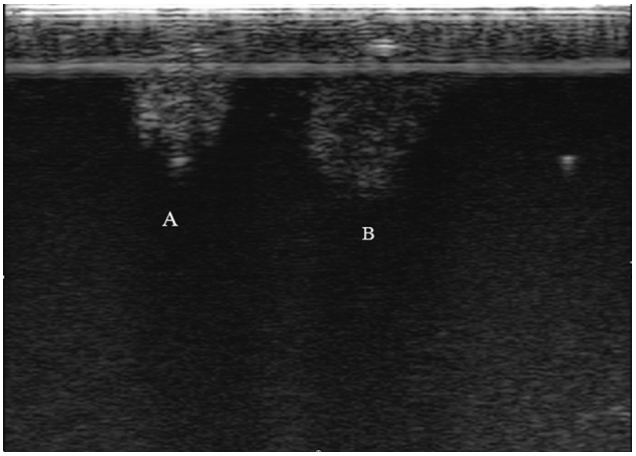

Figure 2. Imaging effort of the microbubble *in vitro*.
A: normal microbubble Sono Vue; B: the targeted microbubble SonoVue-TM.

sinus renalis showed a relatively lower enhancement. The intensity of the contrast agent faded away after it reached the peak value. As the ordinary microbubble administrated in the kidney of Wistar rats, the echo intensity of the medulla nephrica was slight lower than the renal cortex. The clarification order of the contrast agent was sinus renalis, medulla nephrica and renal cortex namely. While the SonoVue-TM microbubble was administrated, the imaging condition showed no significant differences with the ordinary contrast agent, and the echo intensity of the medulla nephrica was lower than the renal cortex. The clarification order of the contrast agent was sinus renalis, medulla nephrica and renal cortex namely. After ordinary microbubble was injected into the GK rat, the echo intensity of the medulla nephrica was slight above the intensity of the renal cortex. The condition of the clarification order was the same as the Wistar rat. When the SonoVue-TM microbubble was used, the echo intensity of the medulla nephrica was significantly higher than the renal cortex. The clarification order of the contrast agent is renal cortex, medulla nephrica and sinus renalis respectively.

3.3. TIC curve of the kidney image

TIC curves of the rat kidney images were all an asymmetric monopeak curves with ascending branch, summit and descending branch. The ascending branch was steep, and the descending branch was flat. The peek value of the ordinary microbubble in renal cortex of Wistar rat was slightly above the medulla nephrica (Figure 3A, B), and the peek value of the ordinary microbubble in renal cortex of GK rat was slightly lower than medulla nephrica (Figure 3C, D). The peek value of the SonoVue-TM microbubble in renal cortex of Wistar rat was slightly above the medulla nephrica (Figure 4A, B), and the peek

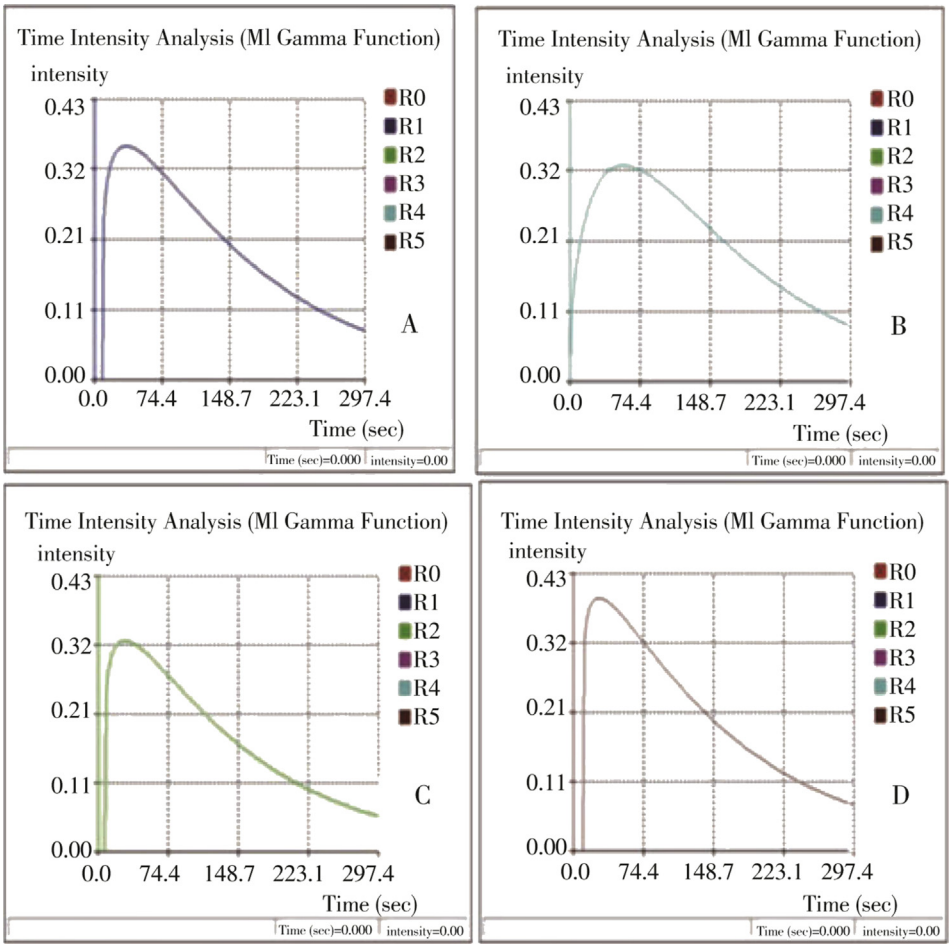

Figure 3. TIC of kidney image after perfusion of microbubble SonoVue.
A: Fitting curve of renal cortex when normal microbubble SonoVue was used in the Wistar rats; B: Fitting curve of renal medulla when normal microbubble SonoVue was used in the Wistar rats; C: Fitting curve of renal cortex when normal microbubble SonoVue was used in the GK rats; D: Fitting curve of renal medulla when normal microbubble SonoVue was used in the GK rats.

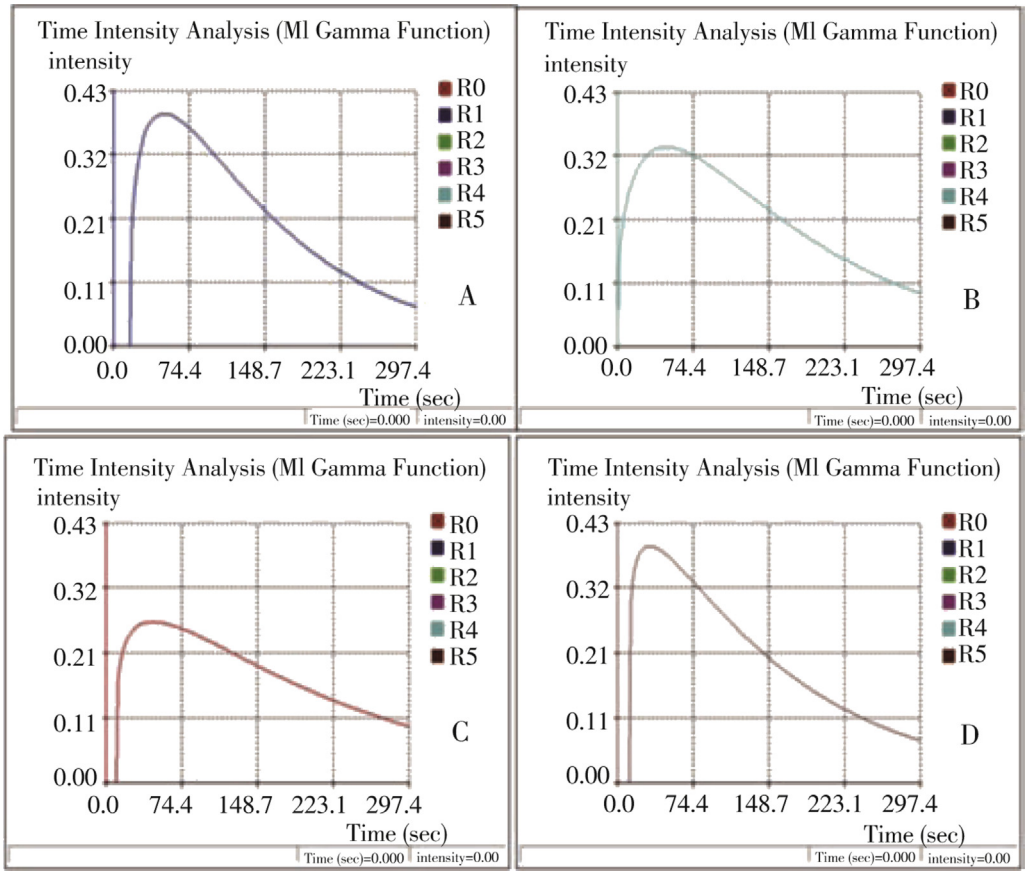

Figure 4. TIC of kidney image after perfusion of targeted microbubble SonoVue-TM.
A: The fitting curve of renal cortex when the targeted microbubble SonoVue-TM was used in the Wistar rats; B: The fitting curve of renal medulla when the targeted microbubble SonoVue-TM was used in the Wistar rats; C: The fitting curve of renal cortex when the targeted microbubble SonoVue-TM was used in the GK rats; D: The fitting curve of renal medulla when the targeted microbubble SonoVue-TM was used in the GK rats.

Table 1
Imaging parameter of rat kidney.

Indexes		Wistar rat		GK rat	
		Renal cortex	Medulla nephrica	Renal cortex	Medulla nephrica
Normal group	S1	0.004 ± 0.002	0.005 ± 0.001	0.007 ± 0.003	0.009 ± 0.003
	S2	−0.001 ± 0.000	−0.001 ± 0.000	−0.001 ± 0.000	−0.001 ± 0.000
	PI	0.306 ± 0.076	0.312 ± 0.036	0.343 ± 0.059	0.387 ± 0.053
	AUC	59.037 ± 18.821	52.749 ± 8.210	62.283 ± 13.183	64.926 ± 12.700
	TTP	47.306 ± 13.433	38.127 ± 10.537	35.153 ± 11.780	36.106 ± 13.324
Targeted group	S1	0.006 ± 0.001*	0.006 ± 0.003*	0.011 ± 0.003*	0.011 ± 0.004*
	S2	−0.001 ± 0.000	−0.001 ± 0.000	−0.001 ± 0.000	−0.001 ± 0.000
	PI	0.359 ± 0.022	0.349 ± 0.045*	0.372 ± 0.028	0.445 ± 0.034*
	AUC	70.694 ± 10.810	63.301 ± 9.728*	68.628 ± 10.312	78.334 ± 12.600*
	TTP	33.967 ± 15.735	44.402 ± 13.848	33.217 ± 16.370	33.213 ± 12.426

S1: the slope of the ascending branch; S2: the slope of the descending branch; PI: the intensity of the peak value; AUC: area under the curve; TTP: time to peak. *$P < 0.05$ compared with normal group.

Table 2
Imaging parameter of GK rat kidney.

Indexes		Normal microbubble SonoVue		Targeted microbubble SonoVue-TM	
		Renal cortex	Medulla nephrica	Renal cortex	Medulla nephrica
Normal group	S1	0.007 ± 0.003	0.009 ± 0.003	0.011 ± 0.003	0.011 ± 0.004
	S2	−0.001 ± 0.000	−0.001 ± 0.000	−0.001 ± 0.000	−0.001 ± 0.000
	PI	0.343 ± 0.059	0.387 ± 0.053	0.372 ± 0.028	0.445 ± 0.034
	AUC	62.283 ± 13.183	64.926 ± 12.700	68.628 ± 10.312	78.334 ± 12.600
	TTP	35.153 ± 11.780	36.106 ± 13.324	33.217 ± 16.370	33.213 ± 12.426
Targeted group	S1	0.004 ± 0.002	0.005 ± 0.001	0.006 ± 0.001	0.006 ± 0.003
	S2	−0.001 ± 0.000	−0.001 ± 0.000	−0.001 ± 0.000	−0.001 ± 0.000
	PI	0.306 ± 0.076	0.312 ± 0.036*	0.359 ± 0.022	0.349 ± 0.045*
	AUC	59.037 ± 18.821	52.749 ± 8.210*	70.694 ± 10.810	63.301 ± 9.728*
	TTP	47.306 ± 13.433	38.127 ± 10.537	33.967 ± 15.735	44.402 ± 13.848

S1: the slope of the ascending branch; S2: the slope of the descending branch; PI: the intensity of the peak value; AUC: area under the curve; TTP: time to peak. *$P < 0.05$ compared with normal group.

value of the ordinary microbubble in renal cortex of GK rat was slightly lower than medulla nephrica (Figure 4C, D).

3.4. Analysis of the kidney image parameter

Compared with the control group, the slope, peek value and the area under the curve of the ascending branch in the renal cortex and the medulla nephrica of GK rat in the ordinary contrast agent group and the SonoVue-TM microbubble group were all improved significantly ($P < 0.05$, Table 1). The slope, peek value and the area under the curve of the ascending branch in the renal cortex and the medulla nephrica of Wistar rat in the ordinary contrast agent group and the SonoVue-TM microbubble group showed no significant difference ($P > 0.05$, Table 2).

4. Discussion

The major cause in pathological and physiological basis of diabetic complications is microcirculation disturbance [8]. The previous study showed that, the change of the microvascular disease was always fundamentally, and the change was reversible. As the disease progressed, the abnormal glucose metabolism made the pathologic changes of the blood vessel irreversible, and this may lead to more serious consequences [9,10]. If evidence of early microvascular disease can be detected, and effective intervention was taken at the reversible period, the progressive vasculopathy will be prevented, and complications will greatly be reduced. In this study, targeted microbubble SonoVue-TM was prepared. By injecting the microbubble into Wistar rat and GK rat, the kidney blood perfusion was observed and compared. The results showed that the targeted microbubble can enhance the imaging ability both *in vitro* and *in vivo*, and reflect the characteristics of the kidney blood perfusion of the GK rat.

The basic concept of ultrasound targeted contrast imaging is to attach the specific antibody or ligand to microbubble [11,12]. The ultrasound microbubble used in this study is an ideal tracer of the microcirculation which belongs to the second generation ultrasound microbubble contrast agents. The microbubble had a lecithoid monolayer, and was filled with sulfur hexafluoride inside. The average diameter is about 2.5 μm, and the stability of the microbubble is favorouble [13,14]. We used Wu Juefei's avidin-biotin bridge method for reference, successfully connected the specific antibody with the microbubble. The results showed that the targeted microbubble SonoVue-TM can image well *in vitro*. The technique has been wildly used in the medicine field with high specificity affinity and stability [15,16].As the ordinary microbubble and the targeted microbubble SonoVue-TM administrated in the kidney of GK rats, the slope of the superior branchlets and the area under the curve all increased, peak intensity enhanced according to the parameter analysis [17]. These results all suggested that the blood flow and velocity increased in the renal microvascular of GK rats, and the renal hemodynamic was abnormal which showed up as high perfusion and high filtration in the GK rats. The result was similar with the previous reports of renal microcirculation in diabetic nephropathy [18]. Compared with the normal microbubble, the targeted microbubble SonoVue-TM showed no significant differences when used in Wistar rats, and this proved that the targeted microbubble SonoVue-TM have no specific retention in the renal of Wistar rats. Compared with the normal microbubble group, the echo intensity of the targeted microbubble SonoVue-TM group was much higher in the renal medulla area than in the cortex area. In targeted microbubble SonoVue-TM group, the peak intensity enhanced obviously, and the area under the curve increased in the renal medulla of the GK rats according to the parameter analysis; while in the normal microbubble group, the echo intensity in the renal medulla area was slightly higher than in the cortex area. There were several possible reasons for the above phenomenon: ① the expression level of TM antigen in the renal medulla of GK rats was higher than Wistar rats; the targeted microbubble SonoVue-TM specifically retained in the microvascular, which enhanced the back scattered reflection echo signal and resulted in the peek value intensity of renal medulla area obviously higher than the cortex area. ② This might be related to the change of blood distribution in the kidney of GK rats, which manifested as the increasement of blood flow in the renal medulla area and decreasement in the cortex area. This phenomenon was similar with the change of renal hemodynamics in acute hemorrhagic shock, which showed up as the decreasing of blood flow in renal cortex, and the non-decreasing (even increasing) of blood flow in medulla area [19]. The level of plasma endothelin in diabetic patient was higher than normal person, especially in those with microvascular complication [20]. Endothelin can constricts blood vessels in renal cortex by ET-A receptor, and at the same time dilates blood vessels in renal medulla by ET-B receptor [21,22]. In addition, the expression level of inducible nitric oxide synthase in the renal tissue of diabetes improved, and then excess nitric oxide was catalyzed [23,24]. The nitric oxide in turn can dilates the blood vessel of glomerular arterioles in the superficial layer of renal cortex, while have no effort on efferent arteriole in the superficial layer of renal medulla [25]. But as it showed an arteriolar vasodilation in juxtamedullary glomerulus, the blood flow in the renal medulla increased respectively. Besides, nitric oxide can mediate the renal medulla vasodilation through endothelin [26]; the level of andrenin-angiotensin will improve in the renal tissue and the blood vessels constricted obviously with diabetes, while nephrons near the medulla are relatively insensitive to andrenin-angiotensin. The mechanism above all can explain why the blood flow in the renal medulla is higher than in the renal cortex in diabetic patient.

In conclusion, the targeted microbubble SonoVue-TM can imaged well *in vitro* and *in vivo*, the imaging time can meet the time limit of ultrasonography, the imaging intensity can also meet the requirement of ultrasonography, and the change of renal blood perfusion in GK rats also can be reflected when the targeted microbubble SonoVue-TM was used in the ultrasonography. But our work is far from enough, for example, effective method to detect the microbubble attached on the endothelial cells has not found yet, which means further study should be done to distinguish the microbubble in circulation or adhere to the target tissue.

Conflict of interest statement

We declare that we have no conflict of interest.

References

[1] Fleischer J, Cichosz SL, Jakobsen PE, Yderstraede K, Gulichsen E, Nygaard H, et al. The degree of autonomic modulation is

associated with the severity of microvascular complications in patients with type I diabetes. *J Diabetes Sci Technol* 2015; **9**(3): 681-686.

[2] Anderson CR, Hu X, Tlaxca J, Tlaxca J, Declèves AE, Houghtaling R, et al. Ultrasound molecular imaging of tumor angiogenesis with an integrin targeted microbubble contrast agent. *Invest Radiol* 2011; **46**(4): 215-224.

[3] Chow AM, Tan M, Gao DS, Fan SJ, Cheung JS, Qiao Z, et al. Molecular MRI of liver fibrosis by a peptide-targeted contrast agent in an experimental mouse model. *Invest Radiol* 2013; **48**(1): 46-54.

[4] McEwan C, Fowley C, Nomikou N, McCaughan B, McHale AP, Callan JF. Polymeric microbubbles as delivery vehicles for sensitizers in sonodynamic therapy. *Langmuir* 2014; **30**(49): 14926-14930.

[5] Hastings NE, Feaver RE, Lee MY, Wamhoff BR, Blackman BR. Human IL-8 regulates smooth muscle cell VCAM-1 expression in response to endothelial cells exposed to atheroprone flow. *Arterioscler Thromb Vasc Biol* 2009; **29**(5): 725-731.

[6] Vercellotti GM, Moldow CF, Jacob HS. Complement, oxidants, and endothelial injury: how a bedside observation opened a door to vascular biology. *J Clin Invest* 2012; **122**(9): 3044-3045.

[7] Greineder CF, Chacko AM, Zaytsev S, Zern BJ, Carnemolla R, Hood ED, et al. Vascular immunotargeting to endothelial determinant ICAM-1 enables optimal partnering of recombinant scFv-thrombomodulin fusion with endogenous cofactor. *PloS One* 2013; **8**(11): e80110.

[8] Jarnert C, Kalani M, Rydén L, Böhm F. Strict glycaemic control improves skin microcirculation in patients with type 2 diabetes: a report from the Diabetes mellitus And Diastolic Dysfunction (DADD) study. *Diabetes Vasc Dis Res* 2012; **9**(4): 287-295.

[9] Munch IC, Larsen M, Kessel L, Borch-Johnsen K, Lund-Andersen H, Glümer C. Cumulative glycemia and microangiopathy in subjects with impaired glucose regulation in the Inter99 study. *Diabetes Res Clin Pract* 2011; **91**(2): 226-232.

[10] van der Zijl NJ, Serné EH, Goossens GH, Moors CC, Ijzerman RG, Blaak EE, et al. Valsartan-induced improvement in insulin sensitivity is not paralleled by changes in microvascular function in individuals with impaired glucose metabolism. *J Hypertens* 2011; **29**(10): 1955-1962.

[11] Williams R, Hudson JM, Lloyd BA, Sureshkumar AR, Lueck G, Milot L, et al. Dynamic microbubble contrast-enhanced US to measure tumor response to targeted therapy: a proposed clinical protocol with results from renal cell carcinoma patients receiving antiangiogenic therapy. *Radiology* 2011; **260**(2): 581-590.

[12] Warram JM, Sorace AG, Saini R, Umphrey HR, Zinn KR, Hoyt K. A triple-targeted ultrasound contrast agent provides improved localization to tumor vasculature. *J Ultrasound Med* 2011; **30**(7): 921-931.

[13] Partovi S, Loebe M, Aschwanden M, Baldi T, Jäger KA, Feinstein SB, et al. Contrast-enhanced ultrasound for assessing carotid atherosclerotic plaque lesions. *AJR Am J Roentgenol* 2012; **198**(1): W13-W19.

[14] Qin S, Caskey CF, Ferrara KW. Ultrasound contrast microbubbles in imaging and therapy: physical principles and engineering. *Phys Med Biol* 2009; **54**(6): R27-R57.

[15] Deelman LE, Declèves AE, Rychak JJ, Sharma K. Targeted renal therapies through microbubbles and ultrasound. *Adv Drug Deliv Rev* 2010; **62**(14): 1369-1377.

[16] Takahashi S, Sato K, Anzai J. Layer-by-layer construction of protein architectures through avidin–biotin and lectin–sugar interactions for biosensor applications. *Anal Bioanal Chem* 2012; **402**(5): 1749-1758.

[17] Oeltze S, Doleisch H, Hauser H, Muigg P, Preim B. Interactive visual analysis of perfusion data. *IEEE Trans Vis Comput Graph* 2007; **13**(16): 1392-1399.

[18] Cheng H, Harris RC. Renal endothelial dysfunction in diabetic nephropathy. *Cardiovasc Hematol Disord Drug Targets* 2014; **14**(1): 22-33.

[19] Raghuraman G, Kalari A, Dhingra R, Prabhakar NR, Kumar GK. Enhanced neuropeptide Y synthesis during intermittent hypoxia in the rat adrenal medulla: role of reactive oxygen species–dependent alterations in precursor peptide processing. *Antioxid Redox Signal* 2011; **14**(7): 1179-1190.

[20] Ergul A. Endothelin-1 and diabetic complications: focus on the vasculature. *Pharmacol Res* 2011; **63**(6): 477-482.

[21] Miyauchi Y, Jesmin S, Sakai S, Kamiyama J, Shimojo N, Rahman A, et al. Effects of selective endothelin (ET)-a receptor antagonist versus dual ET-A/B receptor antagonist on hearts of streptozotocin-treated diabetic rats. *Life Sci* 2014; **111**(1–2): 6-11.

[22] Campia U, Tesauro M, Di Daniele N, Cardillo C. The vascular endothelin system in obesity and type 2 diabetes: pathophysiology and therapeutic implications. *Life Sci* 2014; **118**(2): 149-155.

[23] Youn JY, Gao L, Cai H. The p47phox-and NADPH oxidase organiser 1 (NOXO1)-dependent activation of NADPH oxidase 1 (NOX1) mediates endothelial nitric oxide synthase (eNOS) uncoupling and endothelial dysfunction in a streptozotocin-induced murine model of diabetes. *Diabetologia* 2012; **55**(7): 2069-2079.

[24] Feng MG, Prieto MC, Navar LG. Nebivolol-induced vasodilation of renal afferent arterioles involves β3-adrenergic receptor and nitric oxide synthase activation. *Am J Physiol Renal Physiol* 2012; **303**(5): F775-F782.

[25] Ge Y, Lu Y, Reckelhoff JF. Testosterone dilates renal afferent arteriole via a nitric oxide-mediated mechanism. *FASEB J* 2011; **25**: 837.8.

[26] Abassi Z, Gurbanov K, Rubinstein I, Better OS, Hoffman A, Winaver J. Regulation of intrarenal blood flow in experimental heart failure: role of endothelin and nitric oxide. *Am J Physiol* 1998; **274**(4 Pt 2): F766-F774.